[2] For bisubstrate inhibition, see also K. Hinterding, P. Hagenbuch, J. Rétey, H. Waldmann, *Chem. Eur. J.* **1999**, *5*, 227 – 236.
[3] a) P. T. Männistö, S. Kaakkola, *Pharmacol. Rev.* **1999**, *51*, 593 – 628; b) P. T. Männistö, I. Ulmanen, K. Lundström, J. Taskinen, J. Tenhunen, C. Tilgmann, S. Kaakkola, *Prog. Drug Res.* **1992**, *39*, 291 – 350.
[4] B. Masjost, P. Ballmer, E. Borroni, G. Zürcher, F. K. Winkler, R. Jakob-Roetne, F. Diederich, *Chem. Eur. J.* **2000**, *6*, 971 – 982.
[5] J. Vidgren, L. A. Svensson, A. Liljas, *Nature* **1994**, *368*, 354 – 358.
[6] For earlier approaches to the development of bisubstrate inhibitors for COMT, see E. K. Yau, J. K. Coward, *J. Org. Chem.* **1990**, *55*, 3147 – 3158.
[7] B. Masjost, PhD thesis, ETH Zürich, **2000**.
[8] The MOLOC program with the MAB force field: P. R. Gerber, K. Müller, *J. Comput.-Aided Mol. Des.* **1995**, *9*, 251 – 268.
[9] R. S. Tipson, L. B. Townsend, *Nucleic Acid Chem.* **1978**, *3*, 765 – 769.
[10] All new compounds were fully characterized by IR, ^{1}H and ^{13}C NMR, MS, and elemental analysis or high-resolution MS.
[11] J. A. Montgomery, A. G. Laseter, K. Hewson, *J. Heterocycl. Chem.* **1974**, *11*, 211 – 214.
[12] D. Crich, X.-S. Mo, *Synlett* **1999**, 67 – 68.
[13] R. E. Ireland, L. Liu, *J. Org. Chem.* **1993**, *58*, 2899.
[14] O. Mitsunobu, *Synthesis* **1981**, 1 – 28.
[15] X-ray data for **9**: $C_{23}H_{22}N_6O_5$, $M_r = 462.5$, monoclinic, space group $P2_1$, $\rho_{calcd} = 1.40\ g\,cm^{-3}$, $Z = 2$, $a = 6.933(5)$, $b = 8.12(1)$, $c = 19.48(5)$ Å, $\beta = 91.86(14)^\circ$, $V = 1096(3)$ Å^3, $T = 293$ K. Picker-Stoe diffractometer, $Cu_{K\alpha}$ radiation, $\lambda = 1.5418$ Å. Prismatic crystals (ca. $0.4 \times 0.1 \times 0.015$ mm) were obtained by slow evaporation of a solution of **9** in MeCN. The structure was solved by direct methods (SHELXTL). All heavy atoms were refined anisotropically, H-atoms were fixed isotropically with atomic positions based on stereochemical considerations. Final $R(F) = 0.042$ for 873 reflections with $I > 2\sigma(I)$, $wR(F^2) = 0.11$ for all 1205 data and 308 parameters. Crystallographic data (excluding structure factors) for the structure reported in this paper have been deposited with the Cambridge Crystallographic Data Centre as supplementary publication no. CCDC-166783. Copies of the data can be obtained free of charge on application to CCDC, 12 Union Road, Cambridge CB2 1EZ, UK (fax: (+44) 1223-336-033; e-mail: deposit@ccdc.cam.ac.uk).
[16] G. Zürcher, M. Da Prada, *J. Neurochem.* **1982**, *38*, 191 – 195. Enzyme preparations were preincubated for 15 min at 37 °C with inhibitor concentrations varying from 10^{-4} to 10^{-9} mol L^{-1}. The reaction was started by adding substrate (1,2-benzenediol, $K_M = 357$ μM[4]) and ^{1}[H]/^{3}[H]SAM ($K_M = 33$ μM[4]), reaching a final substrate concentration of 2.5 mM and a final ^{1}[H]/^{3}[H]SAM concentration of 183 μM. The reaction was stopped after incubating the vials for 15 min at 37 °C by adding acetic acid and 2-methoxyphenol (guaiacol).
[17] Crystals of recombinant rat liver COMT[5] were grown by the vapor diffusion method in space group $P3_221$ with cell axes $a = b = 50.6$, $c = 167.7$ Å. The reservoir solution was 25% polyethylene glycol (PEG) 8000, 100 mM ammonium sulfate, and 100 mM bis-Tris pH 5.5 (Tris = tris(hydroxymethyl)aminomethane). The hanging drop consisted of 1 μL of the reservoir solution and 3 μL of a solution containing 10 mg mL^{-1} COMT, 5 mM $MgCl_2$, and 1.6 mM **3**. A data set to 2.6 Å resolution with an R_{sym} value of 5.4% and a completeness value of 97.8% was collected using $Cu_{K\alpha}$ radiation from a rotating anode source. In the highest resolution shell the R_{sym} value was 27.9% and the completeness value of 95.4%. The starting model for refinement was the protein portion of an isomorphous quarternary COMT inhibitor complex in the crystal (F. K. Winkler, F. Hoffmann – La Roche, Basel, unpublished results, **1994**). The structure was completed using MOLOC[8] and refined with CNX (A. T. Brünger, P. D. Adams, G. M. Clore, W. L. DeLano, P. Gros, R. W. Grosse-Kunstleve, J. S. Jiang, J. Kuszewski, M. Nilges, N. S. Pannu, R. J. Read, L. M. Rice, T. Simonson, G. L. Warren, *Acta Crystallogr. Sect. D* **1998**, *54*, 905 – 921) to an *R* factor of 22.3% and a free *R* factor of 28.0%. The refined model consists of protein residues 3 to 214, a Mg^{2+} ion, 16 water molecules, and **3**. 88.8% of the residues are in the most favored regions of the Ramachandran plot. The atomic coordinates have been deposited to the Brookhaven Protein Databank, with the PDB entry code 1JR4.

A Blue Luminescent Star-Shaped Zn^{II} Complex that Can Detect Benzene**

Jun Pang, Eric J.-P. Marcotte, Corey Seward, R. Stephen Brown,* and Suning Wang*

Luminescent metal complexes are a fascinating class of molecules that have found applications in many areas of chemistry and materials science. For example, it has been demonstrated that luminescent metal compounds can function as emitters in light-emitting devices.[1] Luminescence is often used as a tool for the detection of a certain weak metal – metal interactions.[2] There are several recent reports on the effect of organic solvents on the luminescence of transition metal compounds,[2] of which most intriguing are the reports by Balch and co-workers that describe an unusual solvoluminescent phenomenon displayed by gold(I) cluster compounds.[2c,d] The high sensitivity of the luminescence of metal complexes to their environment demonstrated in these reports makes such complexes possible fluorescent sensors for specific chemicals. Although there are abundant reports on the use of luminescent transition metal compounds as fluorescent sensors, information on the direct correlation between structures and sensor capability is still scarce. Blue luminescent compounds are a class of highly sought-after materials primarily, because of their potential application as emitters in electroluminescence displays.[3–4] In addition, because most blue emitters have absorption bands in the UV or near-UV region where many aromatic molecules absorb, they have the potential to function as fluorescent sensors for the detection of aromatic molecules, such as benzene, that are an environmental concern.

During our investigation of blue luminescent compounds, we synthesized a new class of blue luminescent organic star-shaped molecules that contain either 7-azaindolyl or 2,2′-dipyridylamino groups. Some of the new star-shaped molecules have been found to be promising blue emitters in electroluminescence devices.[4d, 5] Most interestingly, we found that the new star-shaped molecules are capable of coordinating to various metal centers, which results in the formation of novel coordination compounds. Some of these new compounds are capable of selectively detecting specific small molecules by functioning as fluorescent sensors, an example of which, the Zn^{II} complex of 1,3,5-tris(*p*-(2,2′-dipyridylamino)phenyl)benzene (TPDPB), is described herein.

The novel TPDPB ligand was obtained by a two-step synthesis in an overall 68% yield. The first step is based on a literature procedure[6] and the second step uses Ullmann condensation methods[7] (Scheme 1). The TPDPB ligand displays a broad emission band at $\lambda_{max} = 386$ nm in solution

[*] Dr. R. S. Brown, Prof. Dr. S. Wang, Dr. J. Pang, E. J.-P. Marcotte, C. Seward
Department of Chemistry
Queen's University
Kingston, ON, K7L 3N6 (Canada)
Fax: (+1) 613-533-6669
E-mail: browns@chem.queensu.ca, wangs@chem.queensu.ca

[**] This work was supported by the Natural Sciences and Engineering Research Council of Canada and the Xerox Research Foundation.

  0044-8249/01/11321-4166 $ 17.50+.50/0

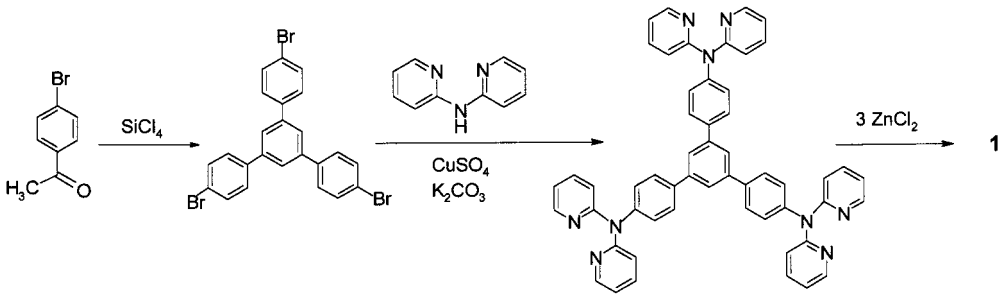

Scheme 1.

(CH_2Cl_2) and at $\lambda_{max} = 400$ nm in the solid state when irradiated by UV light. The quantum efficiency of TPDPB in solution was determined to be 0.19, relative to that of 9,10-diphenylanthracence. The star-shaped complex, $[(ZnCl_2)_3(TPDPB)]$ (**1**) was obtained from the reaction of TPDPB with three equivalents of $ZnCl_2$ in CH_2Cl_2/CH_3OH solution. Complex **1** is stable toward air and moisture in solution and in the solid state, and its fluorescence emission shows an unusually high selectivity to benzene vapor.

Single-crystal X-ray diffraction revealed that **1** adopts several different motifs of crystal lattices,[8] which depend on the solvents used in crystallization. In the presence of CH_2Cl_2 and a small amount of benzene, crystals **A** with the composition of $[(ZnCl_2)_3(TPDPB)] \cdot 3\,CH_2Cl_2 \cdot 0.25\,C_6H_6$ were obtained. When a solution of CH_2Cl_2 and benzene in a 1:1 ratio was used, crystals **B** with the composition of $[(ZnCl_2)_3(TPDPB)] \cdot 3\,C_6H_6$ were formed. The molecular structure of **1** in both crystals is similar. The structure of **1** in the crystal lattice of **A** (Figure 1) has a crystallographically imposed C_3 symmetry with a bowl shape. In both **A** and **B** each $ZnCl_2$ unit is chelated by two 2-pyridyl groups and has a distorted tetrahedral geometry and normal bond lengths[4e, 4f, 9] (**A**: Zn–N 2.017(8) – 2.051(8), Zn–Cl 2.190(3) – 2.198(3) Å; N-Zn-N 90.4(3) – 90.6(3), Cl-Zn-Cl 116.85(16) – 117.24(14), Cl-Zn-N 108.0(2)-116.4(2); **B**: Zn–N 1.969(11)-2.052(9), Zn–Cl 2.148(4) – 2.212(3) Å; N-Zn-N 88.8(5) – 90.1(4), Cl-Zn-Cl 119.58(15) – 122.80(14), Cl-Zn-N 105.2(3) – 116.0(3)°). In the crystal lattice of **A**, two neighboring molecules of **1** are paired and staggered in a face-to-face fashion with the separation between the central phenyl rings being 3.85(1) Å. These pairs stack along the *c* axis to form a hexagonal column. The benzene molecule is situated directly above the central phenyl ring of **1** and sandwiched by two molecules of **1** (Figure 1). The separation between the benzene molecule and the two central phenyl rings of **1** is 3.60(1) Å, indicative of the presence of $\pi - \pi$ stacking interactions. There are three benzene solvent molecules per molecule of **1** in the crystal lattice of **B**, which do not stack with compound **1** in the face-to-face manner observed in **A**. Two of the benzene molecules are nearly perpendicular to the TPDPB ligand while the remaining one is somewhat parallel to the TPDPB ligand shown (Figure 2), but is perpendicular to a neighboring TPDPB ligand of an adjacent molecule in the lattice. The $\pi - \pi$ interactions in **B** are therefore both edge-to-face and face-to-face. The crystals **A** and **B** demonstrate that in the solid state compound **1** has a high affinity for benzene, which makes **1** a possible fluorescent sensor for benzene.

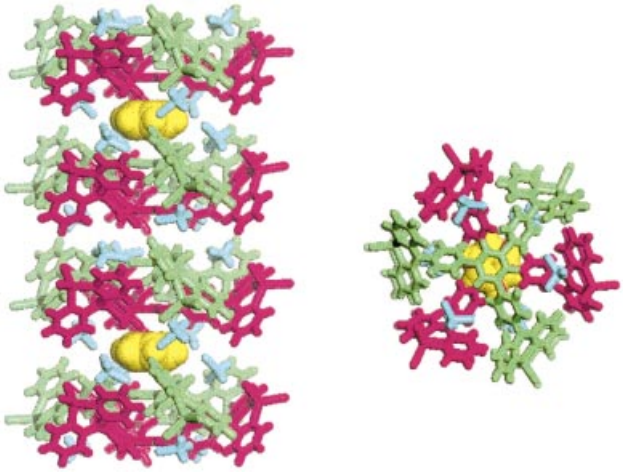

Figure 1. Stick/space-filling diagrams showing the sandwiched arrangement of benzene and **1** in crystal **A**, viewed along *c* axis (left) and viewed down the *c* axis (right). Benzene: yellow, space filling; CH_2Cl_2: light blue, stick. The interlocked pairs of molecules of **1** are shown as red and green, respectively

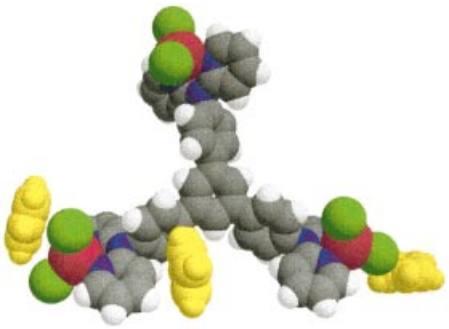

Figure 2. Space-filling diagram of the molecular structure of **1** in crystal **B**. Green: chlorine, blue: nitrogen, red: zinc, gray: carbon, yellow: benzene.

Compound **1** shows a broad emission band ($\lambda_{max} = 417$ nm in solution and $\lambda_{max} = 432$ nm in the solid state) resembling that of TPDPB but red-shifted by ~ 30 nm. A similar red-shift as a consequence of Zn^{II} coordination is observed for tris(2-pyridyl)amine Zn^{II} complexes[4f] where the Zn^{II} ion is chelated by two 2-pyridyl groups in a similar fashion to that in **1**. The quantum efficiency of **1** is similar to that of the free ligand. To study the potential of **1** as a fluorescence sensor, we prepared a modified optical-fiber tip by attaching a freshly prepared prepolymerized polydimethylsiloxane (PDMS) bead containing **1** (1.8 mm diameter, prepared by mixing prepolymerized PDMS (50 mg) with a CH_2Cl_2 (0.3 mL) solution of **1** (0.25 mg) and allowing the mixture to dry until sticky) to a fused silica optical fiber (0.6 mm in diameter). Fluorescent measurements were carried out by using an optical-fiber setup.[10] Upon exposure to benzene, the intensity (integrated) of the

emission band of **1** decreases. The response curves in Figure 3 show both the absolute signal and the Stern–Volmer response. The linear Stern–Volmer response is consistent with well-behaved fluorescence quenching systems. After the removal of benzene vapor, the fluorescence of **1** recovers to the initial intensity. To study the selectivity of our sensor, we

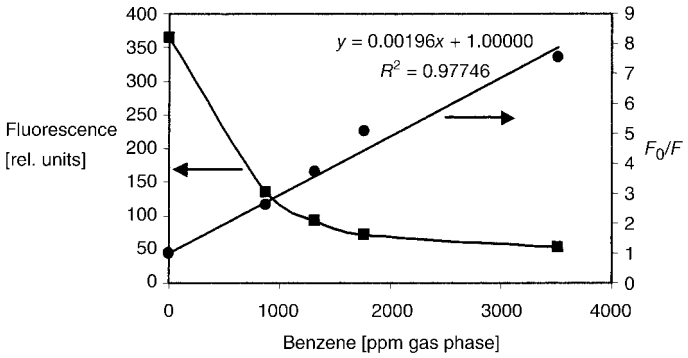

Figure 3. The response curves of **1** as an optical sensor for benzene; F_0/F = Stern–Volmer.

placed our sensor in contact with 500 ppm of selected compounds and examined the change of fluorescent intensity. For each compound, five measurements were carried out. The averaged results given in Figure 4 show that compound **1** has a remarkably high selectivity for benzene. Most noteworthy is that of the four aromatic molecules examined (benzene, toluene, ethyl benzene, and xylene) benzene stands out in terms of fluorescence response. A similar fluorescent response was not observed by using the free ligand TPDPB as the probe.

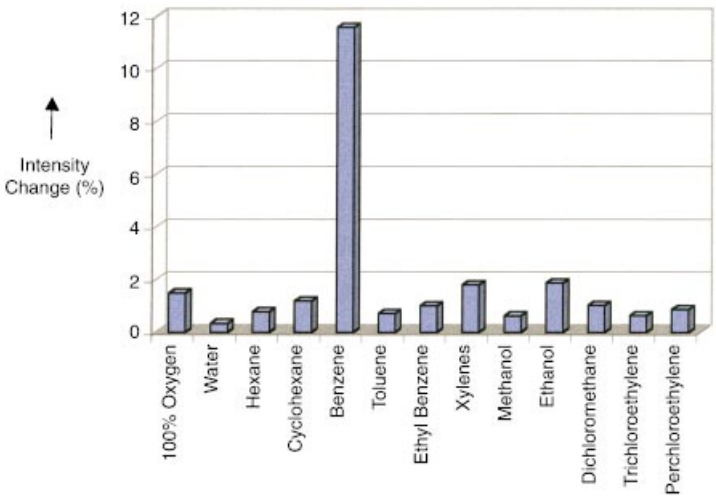

Figure 4. A diagram showing the change of fluorescent intensity of **1** in the optical sensor upon exposure to 500 ppm selected molecules.

Although the precise nature of the interactions between the benzene molecule and compound **1** in PDMS cannot be established at this time, the high selectivity of the fluorescence of compound **1** towards benzene could be attributed to the high affinity of **1** for benzene as demonstrated in the crystals **A** and **B**. Fluorescence quenching by $\pi-\pi$ stacking interactions is well documented.[11] Therefore, $\pi-\pi$ interactions, face-to-face or edge-to-face, between benzene and **1** as observed in **A** and **B** are most likely to be responsible for the fluorescent quenching.

Chemical sensors, based on fiber-optic devices, for benzene have been reported.[12] Fiber-optic sensors based on fluorescence have some advantages over other strategies, these are ease of operation and use, low sensitivity to defects in coatings, insensitivity to electrical interference, and use in gas and liquid phases. However, fluorescence sensors based on solid-state materials for the selective detection of benzene vapor are still rare. Although the response of the optical sensor **1** towards benzene is still far from being suitable for practical applications, it demonstrates that complexes based on the novel TPDPB ligand are promising as fluorescent sensors for specific organic molecules.

Experimental Section

TPDPB: A mixture of 1,3,5-tris-(*p*-bromophenyl)-benzene (0.98 g, 1.8 mmol), 2,2′-dipyridylamine (1.54 g, 9.0 mmol), K_2CO_3 (1.24 g, 9.0 mmol), and $CuSO_4$ (0.13 g, 0.518 mmol) in water (20 mL) and CH_2Cl_2 (100 mL) was stirred well, and evaporated to dryness in vacuum. The residue was heated at 210 °C for 8 h under N_2. After being cooled to ambient temperature, the mixture was dissolved in CH_2Cl_2 (100 mL) and water (100 mL). The organic layer was purified by column chromatography using THF/hexane (3/1) as the eluent to obtain colorless crystalline solid of TPDPB (1.24 g, yield 85 %). M.p. 177–180 °C; ^{1}H NMR (300 MHz, $CDCl_3$, 25 °C): $\delta = 8.42$ (d, $^3J = 5.1$ Hz, 6H, py), 7.79 (s, 3H, ph), 7.71 (d, $^3J = 8.6$ Hz, 6H, ph), 7.63 (dd, $^3J_1 = 8.6$ Hz, $^3J_2 = 6.9$ Hz, 6H, py), 7.32 (d, $^3J = 8.6$ Hz, 6H, ph), 7.08 (d, $^3J = 8.6$ Hz, 6H, py), 7.00 (dd, $^3J_1 = 6.9$ Hz, $^3J_2 = 5.1$ Hz, 6H, py); ^{13}C NMR (300 MHz, $CDCl_3$, 25 °C): $\delta = 158.0$, 148.7, 144.5, 141.7, 138.1, 128.6, 126.9, 118.4, 118.3, 117.8, 117.5. Elemental analysis calcd (%) for $C_{54}H_{39}N_9/H_2O$: C 77.97, H 4.93, N 15.16; found: C 78.51, H 4.75, N 14.64.

1: A solution of TPDPB (0.050 g, 0.0614 mmol) in CH_2Cl_2 (5 mL) was added to a solution of anhydrous $ZnCl_2$ (0.0276 g, 0.203 mmol) in CH_3OH (10 mL) at ambient temperature under N_2. The solution was left to stand for three days and a colorless powder of **1** was obtained (0.066 g, 72 %). M.p. > 300 °C; ^{1}H NMR (300 MHz, [D$_4$]methanol, 25 °C): $\delta = 8.26$ (dd, $^3J = 5.1$ Hz, $^4J = 0.9$ Hz, 6H, py), 7.92 (S, 3H, ph), 7.83 (d, $^3J = 8.4$ Hz, 6H, ph), 7.75 (ddd, $^3J = 7.8$ Hz, $^3J' = 7.2$ Hz, $^4J = 1.8$ Hz, 6H, py), 7.31 (d, $^3J = 8.4$ Hz, 6H, ph), 7.13 (dd, $^3J = 7.2$ Hz, $^3J' = 5.1$ Hz, 6H, py), 7.11 (d, $^3J = 7.8$ Hz, 6H, py). Elemental analysis calcd (%) for $C_{58.5}H_{46.5}N_9Cl_{12}Zn_3$: C 46.93, H 3.13, N 8.42, found: C 46.61, H 2.94, N 8.80.

Received: May 7, 2001
Revised: June 8, 2001 [Z 17060]

[1] a) M. A. Baldo, D. F. O'Brien, Y. You, A. Shoustikov, S. Sibley, M. E. Thompson, S. R. Forrest, *Nature* **1998**, *395*, 151; b) D. F. O'Brien, M. A. Baldo, M. E. Thompson, S. R. Forrest, *Appl. Phys. Lett.* **1999**, *74*, 442; c) R. C. Kwong, S. Sibley, T. Dubovoy, M. Baldo, S. R. Forrest, M. E. Thompson, *Chem. Mater.* **1999**, *11*, 3709; d) R. C. Kwong, S. Laman, M. E. Thompson, *Adv. Mater.* **2000**, *12*, 1134; e) C. H. Chen, J. Shi, *Coord. Chem. Rev.* **1998**, *171*, 161; f) N. X. Hu, M. Esteghamatian, S. Xie, Z. Popovic, A. M. Hor, B. Ong, S. Wang, *Adv. Mater.* **1999**, *11*, 17.

[2] a) M. A. Mansour, W. B. Connick, R. J. Lachicotte, H. J. Gysling, R. Eisenberg, *J. Am. Chem. Soc.* **1998**, *120*, 1329; b) Y. Kunugi, K. R. Mann, L. L. Miller, C. L. Exstrom, *J. Am. Chem. Soc.* **1998**, *120*, 589; c) E. Y. Fung, M. M. Olmstead, J. C. Vickery, A. L. Balch, *Coord. Chem. Rev.* **1998**, *171*, 151; d) J. C. Vickery, M. M. Olmstead, E. Y. Fung, A. L. Balch, *Angew. Chem.* **1997**, *109*, 1227; *Angew. Chem. Int. Ed. Engl.* **1997**, *36*, 1179; e) G. De Santis, L. Fabbrizzi, M. Licchelli, A. Poggi, A. Taglietti, *Angew. Chem.* **1996**, *108*, 224; *Angew. Chem. Int. Ed. Engl.* **1996**, *35*, 202; f) A. P. de Silva, H. Q. N. Gunaratne, T. E.

  0044-8249/01/11321-4168 $ 17.50+.50/0

Rice, *Angew. Chem.* **1996**, *108*, 2253; *Angew. Chem. Int. Ed. Engl.* **1996**, *35*, 2116.

[3] a) C. P. Moore, S. A. VanSlyke, H. J. Gysling (Eastman Kodak), US-A 5484922, **1996**; b) T. Sano, M. Fujita, T. Fujii, Y. Nishio, Y. Hamada, K. Shibata, K. Kuroki (Sanyo Electric Company), US-A 5432014, **1995**; c) Y. Hironaka, H. Nakamura, T. Kusumoto (Idemitsu Kosan Company), US-A 5466392, **1995**; d) S. A. VanSlyke, P. S. Bryan, F. V. Lovecchio (Eastman Kodak), US-A 5150006, **1992**; e) P. S. Bryan, F. V. Lovecchio, S. A. VanSlyke (Eastman Kodak), US-A 5141671, **1992**; f) Y. Hamada, T. Sano, M. Fujta, T. Fujii, Y. Nishio, K. Shibata, *Chem. Lett.* **1993**, 905; g) N. Nakamura, S. Wakabayashi, K. Miyairi, T. Fujii, *Chem. Lett.* **1994**, 1741.

[4] a) J. Ashenhurst, G. Wu, S. Wang *J. Am. Chem. Soc.* **2000**, *122*, 2541; b) J. Ashenhurst, S. Wang, G. Wu *J. Am. Chem. Soc.* **2000**, *122*, 3528; c) Q. Wu, M. Esteghamatian, N. X. Hu, Z. Popovic, G. Enright, S. R. Breeze, S. Wang, *Angew. Chem.* **1999**, *111*, 1039; *Angew. Chem. Int. Ed.* **1999**, *38*, 985; d) Q. Wu, Y. Tao, M. D'Iorio, S. Wang, *Chem. Mater.* **2001**, *13*, 71; e) Q. Wu, J. A. Lavigne, Y. Tao, M. D'Iorio, S. Wang, *Inorg. Chem.* **2000**, *39*, 5248; f) W. Yang, H. Schmider, Q. Wu, Y. Zhang, S. Wang, *Inorg. Chem.* **2000**, *39*, 2397; g) S. Liu, Q. Wu, H. L. Schmider, H. Aziz, N. X. Hu, Z. Popovic, S. Wang, *J. Am. Chem. Soc.* **2000**, *122*, 3671.

[5] J. Pang, Y. Tao, M. D'Iorio, S. Wang, *Chem. Mater.* **2001**, submitted.

[6] S. S. Elmorsy, A. Pelter, K. Smith, *Tetrahedron. Lett.* **1991**, *32*, 4175 – 4176.

[7] a) H. B. Goodbrand, N. X. Hu, *J. Org. Chem.*, **1999**, *64*, 670; b) J. Lindley, *Tetrahedron* **1984**, *40*, 1433; c) P. E. Fanta, *Synthesis* **1974**, 1.

[8] Crystal data for crystal **A**: $C_{54}H_{39}N_9Cl_6Zn_3 \cdot 3CH_2Cl_2 \cdot 0.25C_6H_6$, rhombohedral, $R\bar{3}$, $a = b = 33.517(4)$, $c = 19.167(3)$ Å, $V = 18647(4)$ Å^3, $Z = 12$. Crystal data for crystal **B**: $C_{54}H_{39}N_9Cl_6Zn_3 \cdot 3C_6H_6$, triclinic, $P\bar{1}$, $a = 13.805(4)$, $b = 14.848(5)$, $c = 17.384(5)$ Å, $\alpha = 87.208(6)$, $\beta = 88.569(6)$, $\gamma = 77.828(8)^\circ$, $V = 3478.7(18)$ Å^3, $Z = 2$. Data were collected on a Bruker CCD1000 X-ray diffractometer at 24 °C. Structural solution and refinements were carried out using Bruker AXS SHELXTL NT software. Convergence to final $R_1 = 0.1283$ and $wR_2 = 0.3320$ by using 10089 reflections and 495 parameters for **A** and $R_1 = 0.0991$ and $wR_2 = 0.1079$ by using 16047 reflections and 791 parameters for **B** were achieved. Crystallographic data (excluding structure factors) for the structures reported in this paper have been deposited with the Cambridge Crystallographic Data Centre as supplementary publication no. CCDC-163379 (**A**) and -163380 (**B**). Copies of the data can be obtained free of charge on application to CCDC, 12 Union Road, Cambridge CB2 1EZ, UK (fax: (+44) 1223-336-033; e-mail: deposit@ccdc.cam.ac.uk).

[9] a) R. H. Prince in *Comprehensive Coordination Chemistry*, *Vol. 5.* (Eds.: G. Wilkinson, R. D. Gillard, J. A. McCleverty), Pergamon, New York, **1987**, chap. 56.1; b) T. P. E. Auf der Heyde, *Acta Crystallogr. Sect. B* **1984**, *40*, 582; c) M. C. Kerr, H. S. Preston, H. L. Ammon, J. E. Huheey, J. M. Stewart, *J. Coord. Chem.* **1981**, *11*, 111; d) H. W. Smith, *Acta Crystallogr. Sect. B* **1975**, *31*, 2701.

[10] Fluorescence emission was measured by coupling the modified fiber to a miniature optical-fiber based spectrometer (SF2000, Ocean Optics, Dunedin, FL), which consists of a fixed grating and charge coupled device (CCD) array detector that covers a spectral range of 300 to 1000 nm. An UV light-emitting diode (368 nm, Nichia, San Jose, CA) was used for excitation. The fiber tip was inserted into a 1.1 L sealed flask, and appropriate volumes of various solvent liquids added and allowed to evaporate for gas-phase exposure.

[11] a) S. Bevers, S. Schutte, L. W. McLaughlin, *J. Am. Chem. Soc.* **2000**, *122*, 5905; b) K. Shirai, M. Matsuoka, K. Fukunishi, *Dyes Pigm.* **1999**, *42*, 95; c) M. Balon, P. Guardado, M. A. Munoz, C. Carmona, *Biospectroscopy* **1998**, *4*, 185; d) J. S. Hinzmann, R. L. McKenna, T. S. Pierson, F. Han, F. J. Kezdy, D. E. Epps, *Chem. Phys. Lipids* **1992**, *62*, 123.

[12] a) A. Abdelghani, J. M. Chovelon, N. Jaffrezic Renault, C. Veilla, H. Gagnaire, *Anal. Chim. Acta* **1997**, *337*, 225; b) R. Angelucci, A. Poggi, L. Dori, A. Tagliani, G. C. Cardinali, F. Corticelli, M. Marisaldi, *J. Porous Mater.* **2000**, *7*, 197.

Lamellae-Nanotube Isomerism in Hydrogen-Bonded Host Frameworks**

Matthew J. Horner, K. Travis Holman, and Michael D. Ward*

The supramolecular organization displayed by surfactant assemblies (SAs) and block copolymers (BCs) is often characterized by various ordered microstructures—spherical, lamellar, hexagonal, and cubic phases—that exhibit different curvatures of a common interface that defines the boundary between dissimilar segments of the molecular components. The ultimate microstructure reflects a delicate balance of forces on opposite sides of the interface.[1, 2] Though typically described by smaller length scales, analogous architectures are evident in crystalline small-molecule assemblies,[3] such as the hexagonal urea[4] and perhydrotriphenylene[5] inclusion compounds, supramolecular hydrogen-bonded nanotubes formed by cyclic peptides[6] and cyclodextrins,[7] high-symmetry metal–organic coordination networks,[8] and lamellar organic salts.[9] To the best of our knowledge, however, structural isomerism in organic single crystals based on the curvature of a common two-dimensional supramolecular interface is unknown.

We previously reported that, depending on the identity of the organic substituent, guanidinium organomonosulfonates typically crystallize as either bilayered or continuously layered (CL) architectures. The organic substituents form interdigitated arrays between "quasihexagonal" hydrogen-bonded sheets of the guanidinium ions (**G**) and sulfonate (**S**) moieties (Figure 1).[10] The two architectures differ with respect to the projection of the organic substituents from each **GS** sheet—whereas substituents project from the same side of each sheet in the bilayer form they project from both sides in the CL architecture, thereby accommodating substituents with a larger steric "footprint". The **GS** sheet can be described as one-dimensional **GS** ribbons fused by hydrogen bond "hinges" that allow the sheets to pucker (about an angle θ_{IR}) in the CL architectures in order to optimize the packing of the organic substituents.[11] Guanidinium salts of appropriately chosen organodisulfonates form analogous bilayer and continuous "brick" host architectures in which the organic substituents serve as "pillars" and generate guest-filled inclusion cavities between the **GS** sheets.[12] The preference for a given host architecture depends upon the shape and relative sizes of the pillars and guests, the latter behaving as templates that direct the formation of a particular **GS** host architecture.

We have now discovered that guanidinium organomonosulfonates can also form inclusion compounds, with their

[*] Prof. Dr. M. D. Ward, M. J. Horner, Dr. K. T. Holman
Department of Chemical Engineering and Materials Science
University of Minnesota
Minneapolis, MN 55445 (USA)
Fax: (+1) 612-626-7805
E-mail: wardx004@tc.umn.edu

[**] This work was supported by the National Science Foundation (DMR-9908627), in part by the MRSEC Program of the National Science Foundation (DMR-9809364), and the Natural Sciences and Engineering Research Council of Canada (postdoctoral fellowship for K.T.H.).